DOT/FAA/AR-97/3

Office of Aviation Research
Washington, D.C. 20591

A Fuel Generation Model For Char Forming Polymers in Fires

Richard E. Lyon

Federal Aviation Administration
Airport and Aircraft Safety
Research and Development Division
William J. Hughes Technical Center
Atlantic City International Airport, NJ 08405

August 1997

Final Report

U.S. Department of Transportation
Federal Aviation Administration

NOTICE

Technical Report Documentation Page

1. Report No.	2. Government Accession No.	3. Recipient's Catalog No.
DOT/FAA/AR-97/3		

4. Title and Subtitle	5. Report Date
A FUEL GENERATION MODEL FOR CHAR FORMING POLYMERS IN FIRES	August 1997
	6. Performing Organization Code: AAR-422

7. Author(s)	8. Performing Organization Report No.
Richard E. Lyon	DOT/FAA/AR-97/3

9. Performing Organization Name and Address	10. Work Unit No. (TRAIS)
Fire Safety Section AAR-422 Federal Aviation Administration William J. Hughes Technical Center Atlantic City International Airport, NJ 08405	11. Contract or Grant No.

12. Sponsoring Agency Name and Address	13. Type of Report and Period Covered
U.S. Department of Transportation Federal Aviation Administration Office of Aviation Research Washington, DC 20591	Final Report
	14. Sponsoring Agency Code

15. Supplementary Notes

16. Abstract

A mass loss model for char forming polymers in fires is developed from mechanistic pyrolysis kinetics. Under conditions of flaming combustion the coupled rate equations for thermal degradation products and reactants reduce to a single rate law for the residual mass. Exact results are obtained from the mass loss history which include an equilibrium char yield whose value depends only on the relative rates of gas and char formation at a particular temperature. Reaction rate constants for thermolysis of chemical bonds, gas production, and char formation are determinable from parametric fits of the mechanistic charring model to thermogravimetric data. Predictions of the nonisothermal mass loss during constant heating rate experiments are in agreement with experimental data over the expected range of validity.

17. Key Words	18. Distribution Statement
Pyrolysis, Kinetics, Polymer, Thermogravimetric analysis, Flammability, Fire	This document is available to the public through the National Technical Information Service (NTIS), Springfield, Virginia 22161.

19. Security Classif. (of this report)	20. Security Classif. (of this page)	21. No. of Pages	22. Price
Unclassified	Unclassified	18	

ACKNOWLEDGMENTS

The author would like to thank Dr. Jonahira R. Arnold, Dr. Sajal Das, and Richard N. Walters for helpful discussions and analyses.

TABLE OF CONTENTS

LIST OF FIGURES

LIST OF TABLES

EXECUTIVE SUMMARY

A fuel generation model for char forming polymers in fires is developed from mechanistic pyrolysis kinetics. Under conditions of flaming combustion the coupled rate equations for thermal degradation products and reactants reduce to a single rate law for the residual mass. Exact results are obtained from the mass loss history which include an equilibrium char yield whose value depends only on the relative rates of gas and char formation at a particular temperature. Reaction rate constants for thermolysis of chemical bonds, gas production, and char formation are determined from parametric fits of the mechanistic charring model to thermogravimetric data. Predictions of the nonisothermal mass loss during constant heating rate experiments are in agreement with experimental data over the expected range of validity.

INTRODUCTION

Full-scale fire tests have demonstrated that the heat release rate of a burning material is the single most important parameter determining its fire hazard in an enclosed environment such as a room [1], submarine [2], rail car [3], or passenger aircraft cabin [4]. Bench-scale fire tests have shown that polymers which form a carbonaceous char during burning have lower ignitability [5] and lower heat release rate than nonchar forming polymers [6]. Char formation in a fire limits the amount of volatile fuel that can be produced by the burning polymer, provides a thermally insulating layer at the surface to reduce heat transmission into the material, and acts as a diffusion barrier to combustible gases. Despite the empirical correlation between char formation and reduced flammability of synthetic polymers [5-7], pyrolysis models which include char formation have focused almost entirely on the naturally occurring polymer cellulose [8-19]. The present work provides a generalized pyrolysis model which accounts for thermally induced gasification and char formation of synthetic polymers and which can be evaluated using standard laboratory thermogravimetric equipment. Analytic solutions having a minimum number of adjustable parameters were pursued in order to provide insight into the solid state thermochemical processes governing polymer combustion and to help guide the search for fire resistant materials for next generation aircraft interiors.

BACKGROUND

The steps involved in the flaming combustion of solid polymers are described schematically in figure 1, after van Krevelen [20]. Flaming combustion requires three coupled processes: heating of the polymer, thermal decomposition/pyrolysis, and ignition of the gaseous decomposition products in air. An ignition source or thermal feedback of radiant energy from the flame supplies heat to the polymer surface which causes thermolytic cleavage of primary chemical bonds in the polymer molecules. Pyrolysis gases mix and react with air in the combustion zone above the surface releasing heat and producing carbon dioxide, water, and incomplete combustion products such as carbon monoxide and soot.

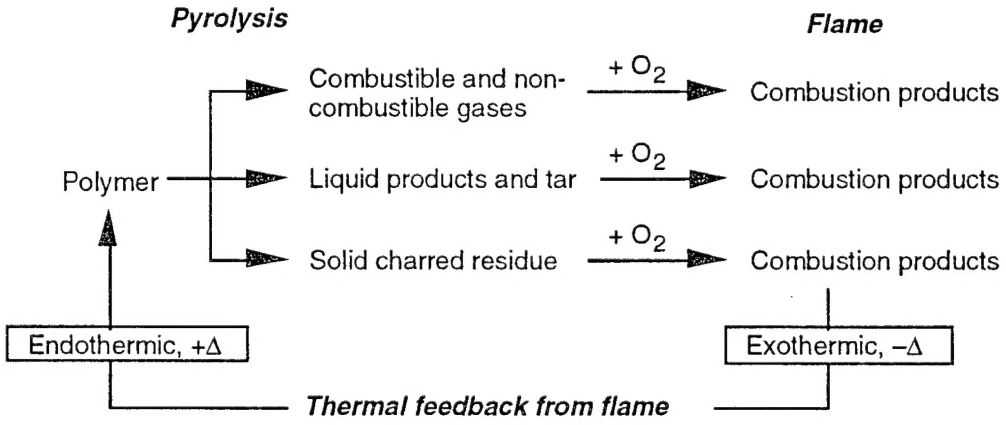

FIGURE 1. SCHEMATIC OF THE COMBUSTION PROCESS OF SOLID POLYMERS AFTER [20]

One-dimensional burning models for polymers have been developed with coupled heat and mass transfer and kinetically controlled thermal decomposition in the pyrolysis zone of the burning material for both charring [16-17] and noncharring polymers [21]. The basic thermal degradation mechanism leading to volatile fuel generation in char forming polymers has been described as a generalized chemical bond scission process consisting of primary and secondary decomposition events [19, 22-24]. The primary decomposition step is main-, end-, or side-chain scission of the

polymer to form free radical intermediates. Subsequent hydrogen transfer and/or recombination of the intermediates lead to primary volatiles (gas and tar) and char. The primary char further decomposes by dehydrogenation to form the secondary gas and a thermally stable secondary char.

Broido and Nelson [9] may have been the first to propose a mechanistic parallel reaction model wherein cellulose thermally decomposes directly to tar and char through competing reactions. The two-step parallel reaction model for cellulose predicted a variable but finite residual mass after pyrolysis which depended on time and temperature (i.e., heating rate) through the magnitude of the rate constants for the competing processes. Lewellen et al. [13] extended the cellulose parallel reaction scheme to include the formation and evaporation of an active intermediate (levoglucosan) which subsequently degrades to tar and char through competing reactions. The introduction of a reactive intermediate by Lewellen qualitatively accounted for the absence of char in rapidly heated (10^2–10^5 K/s) samples where the residence time of the intermediate in the condensed phase was insufficient to allow char formation, i.e., the rate of char formation was slow compared to the rate of evaporation of the reactive intermediate at high temperatures. Suuberg et al. [15] adopted Lewellyn's model of cellulose decomposition but suggested that the first step in the pyrolysis--generation of the reactive intermediate from the parent cellulose--was a reversible process, as suggested for levoglucosan formation [25]. The reversibility of the first step implied a low concentration of the reactive intermediate during the course of the pyrolysis which accounted for the low measured vapor pressures. Moreover, equilibrium between the cellulose and tar intermediate would not be achieved at low temperatures because the intermediate would be rapidly consumed by gasification and charring [15]. Reversible dissociation of the polymer to a reactive intermediate is analogous to the ceiling temperature in polymerization reactions [26].

Suuberg's model suggests that formation of the active tar intermediate is the rate limiting step at temperatures below the tar vaporization temperature ≈ 530-570 K [15, 27], while mass transport of the tars is the rate limiting step at high heating rates and temperatures. A schematic representation of Suuberg's model is

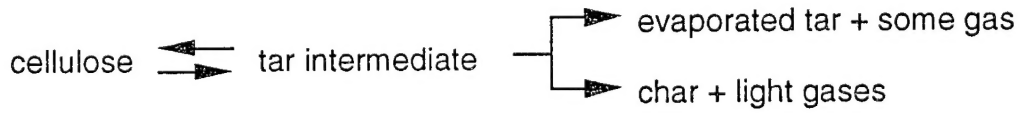

Decomposition schemes which account for some or all of these pyrolysis products have been proposed wherein the decomposition steps occur sequentially (series), simultaneously (parallel), or in some combination of series/parallel steps [9-19]. Three of these mechanistic pyrolytic reaction schemes for cellulose have been reviewed recently [18] including the single-step first order model [17], an uncoupled three-step parallel model [8], and a coupled three-step series-parallel model [9, 19]. The single-step and three-step uncoupled models have a fixed char yield as an adjustable parameter while the three-step coupled model has a variable char yield. All of the models predict rate dependent peak decomposition temperatures. Variable (n-th) order decomposition kinetics have been fit to mass loss data for char forming polymers with reasonable success using reaction order [12, 28] and empirical weighting factors [29] as adjustable parameters. However, little insight is gained into the reaction pathways from these curve-fitting exercises. An analytic solution for the isothermal residual mass of the polymer in the single-step and three-step uncoupled and the n-th order empirical models is possible because the reactions are first order in the polymer mass. The coupled model has been solved analytically for the residual isothermal mass but requires six kinetic parameters and a maximum char yield for evaluation. Numerical solutions of the three-step delinked [16] and parallel models have been published for constant and variable heating rates [18].

POLYMER THERMAL DECOMPOSITION

The condensed phase thermal decomposition pathway of polymers is assumed to be a series-parallel reaction model [9, 19] which includes a reversible first step [15] and secondary char formation [20] as shown in figure 2.

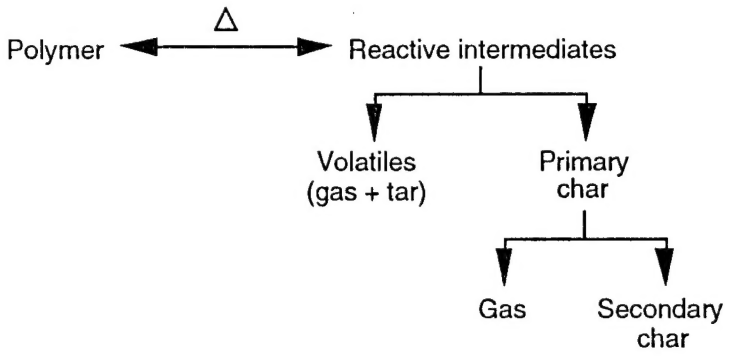

FIGURE 2. SCHEMATIC REPRESENTATION OF PRIMARY AND SECONDARY DECOMPOSITION PROCESSES IN POLYMER PYROLYSIS

Equations 1-5 describe the anaerobic reactions, and equations 6-8 extend the model to include condensed phase oxidation reactions of the reactive intermediate, primary, and secondary char. Bulk and surface oxidation reactions become important for long-term thermoxidative stability and smoldering combustion, respectively. In reactions 1-8, P is the polymer, I* is the reactive intermediate, G1 and C1 are the primary volatiles and char, and G2 and C2 are the secondary gas and char. Solid-state bulk and surface oxidation reaction products for the intermediate, primary char, and secondary char are denoted, I^*O_2, $C1O_2$, and $C2O_2$, respectively.

$$P \underset{k_{-p}}{\overset{k_p}{\rightleftharpoons}} I^* \tag{1}$$

$$I^* \xrightarrow{k_{g1}} G1 \tag{2}$$

$$I^* \xrightarrow{k_{c1}} C1 \tag{3}$$

$$C1 \xrightarrow{k_{g2}} G2 \tag{4}$$

$$C1 \xrightarrow{k_{c2}} C2 \tag{5}$$

$$I^* + O_2 \xrightarrow{k_{I^*O}} I^*O_2 \tag{6}$$

$$C1 + O_2 \xrightarrow{k_{c1O}} C1O_2 \tag{7}$$

$$C2 + O_2 \xrightarrow{k_{c2O}} C2O_2 \tag{8}$$

In equations 1-8, k_p and k_{-p} are the rate constants for the forward and reverse polymer dissociation steps, respectively; k_{g1} and k_{c1} are rate constants for primary gas/tar and char formation; k_{g2} and k_{c2} are the rate constants for secondary gas and char formation; and k_{I*O}, k_{c1O}, and k_{c2O} are the rate constants for the oxidation reactions of the intermediate species and primary and secondary chars in the solid state. Although equations 1–8 represent a highly simplified set of reactions and products, the resulting system of rate equations is highly coupled and an analytic solution in terms of the overall sample mass is impossible.

MASS LOSS KINETICS

The objective of this work is to derive analytic solutions for the mass loss history of a burning polymer from a mechanistically based kinetic model of polymer pyrolysis which accounts for products that are important in the burning process, i.e., combustible gases and char. Of particular interest are simple solutions for the mass loss history of a polymer which provide insight into the mechanisms of decomposition, allow estimation of the fuel generation rate under isothermal and nonisothermal heating, and can be verified using standard laboratory thermogravimetric techniques. To develop the model, assumptions are made about the process of polymer thermal degradation which are relevant to flaming combustion and which will reduce equations 1–8 to a tractable set. The following are proposed:

Assumption A: The breaking of primary chemical bonds in the polymer (thermolysis) [30] is the rate limiting step at heating rates and surface temperatures observed in fires [31], i.e., $P \rightarrow I^*$ is slow compared to the $I^* \rightarrow G1$ and $I^* \rightarrow C1$ reactions which form volatiles and char.

Assumption B: The reactive intermediate I* generated in the polymer dissociation step is in dynamic equilibrium with the parent polymer but is consumed in the process of gas and char formation such that its concentration never becomes appreciable and decreases slowly over time as the polymer is consumed. Consequently, the rate of change of I* with time is insignificant compared to the rate of polymer consumption, gas production, and char formation, so that for computational purposes, $dI^*/dt = 0$. This is the stationary-state hypothesis.

Assumption C: Thermal decomposition of primary char to secondary char and gas, i.e., $C1 \rightarrow C2$ and $C1 \rightarrow G2$, is slow compared to the formation of the primary char $I^* \rightarrow C1$ at typical flaming surface temperatures of 350-700°C. Consequently, only the primary char is considered in formulating the reaction set for the mass loss model.

Assumption D: The thermoxidative environment in the pyrolysis zone of a burning solid polymer is anaerobic. Dissolved molecular oxygen and oxygen diffusion into the pyrolysis zone of the solid are considered negligible with respect to their effects on gas and char formation so that equations 6–8 can be neglected in the kinetic model of polymer combustion. This assumption does not preclude the possibility of surface mass loss due to thermoxidative reactions at the polymer-air interface, e.g., thermogravimetric (TGA) experiments conducted in air or smoldering fires.

In combination with the generalized combustion and pyrolysis schemes of figures 1 and 2, assumptions A–D lead to a simplified mass loss model for polymer combustion which is shown in figure 3. This simplified scheme reduces gas and char formation to a single step involving parallel reactions of the active intermediate, I*.

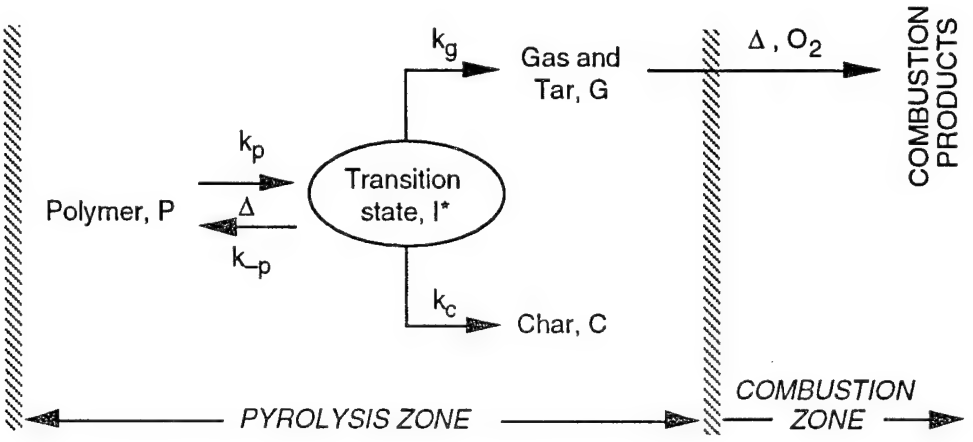

FIGURE 3. KINETIC MODEL FOR POLYMER FLAMING COMBUSTION

The reduced reaction set from figure 3 becomes:

$$P \underset{k_{-p}}{\overset{k_p}{\rightleftharpoons}} I^* \tag{1}$$

$$I^* \xrightarrow{k_g} G \tag{9}$$

$$I^* \xrightarrow{k_c} C \tag{10}$$

and the system of rate equations for the species at time t is

$$\frac{dP}{dt} = -k_p P + k_{-p} I^* \tag{11}$$

$$\frac{dI^*}{dt} = k_p P - \left(k_{-p} + k_g + k_c\right) I^* \tag{12}$$

$$\frac{dG}{dt} = k_g I^* \tag{13}$$

$$\frac{dC}{dt} = k_c I^* \tag{14}$$

According to the stationary-state hypothesis (Assumption B), $dI^*/dt = 0$, so that equation 12 provides the useful result

$$I^* = \left[\frac{k_p}{k_{-p} + k_g + k_c}\right] P = k^* P \tag{15}$$

Substituting $I^* = k^*P$ from equation 15 into equations 11, 13, and 14

$$\frac{dP}{dt} = -\left[k_p - k^* k_{-p}\right] P \tag{16}$$

$$\frac{dG}{dt} = k_g k^* P \tag{17}$$

$$\frac{dC}{dt} = k_c k^* P \tag{18}$$

With $I^* << P$, G, and C the total mass balance in terms of the initial mass, m_o, is:

$$m_o = P + G + C + I^* \approx P + G + C \tag{19}$$

Since $dm_o/dt = 0$, equations 16 and 19 lead to

$$\frac{dP}{dt} = -\frac{dC}{dt} - \frac{dG}{dt} = -\left[k_p - k^* k_{-p}\right] P \tag{20}$$

The sensible mass, m, of the sample as measured, for example, in a TGA experiment or fire calorimeter test is

$$m = P + C + I^* \approx P + C \tag{21}$$

From equations 17 and 20

$$\frac{dm}{dt} = \frac{dP}{dt} + \frac{dC}{dt} = -\frac{dG}{dt} = -k^* k_g P \tag{22}$$

Equation 16 can be solved immediately for P for the initial condition, $P = P_o = m_o$ @ $t = 0$, with the result

$$P = m_o \exp\left(-\left[k_p - k^* k_{-p}\right] t\right) \tag{23}$$

Substituting this result for P into equation 22 and separating variables

$$\int_{m_o}^{m} dm' = -\int_0^t k^* k_g m_o \exp\left(-\left[k_p - k^* k_{-p}\right] \tau\right) d\tau \tag{24}$$

Since k_g and $k_c >> k_p$ and k_{-p} by Assumption A,

$$k_p - k^* k_{-p} = k_p \left| \frac{k_g + k_c}{k_{-p} + k_g + k_c} \right| \approx k_p$$

the solution of equation 24 is

$$\frac{m(t)}{m_o} = 1 - \left[\frac{k_g}{k_g + k_c} \right] \{ 1 - \exp(-k_p t) \} \tag{25}$$

Equation 25 shows that as $t \rightarrow \infty$ the residual mass, m/m_o, approaches an equilibrium value at constant temperature given by

$$\frac{m(\infty)}{m_o} = \left[\frac{k_c}{k_g + k_c} \right] \equiv Y_c \tag{26A}$$

Assuming Arrhenius forms for k_g and k_c,

$$Y_c = Y_c(T) = \left[1 + \frac{A_g}{A_c} \exp\left[-(E_g - E_c)/RT \right] \right]^{-1} \tag{26B}$$

with E_c and E_g and A_c and A_g being the activation energies and frequency factors for char and gas formation, respectively. Equation 26 predicts a finite residual mass at infinite time if $k_c > 0$ and zero residual mass if $k_c = 0$. The physical significance of a temperature dependent, equilibrium, residual mass as the ratio of rate constants for volatile and char formation is consistent with the use of group contributions for the char forming tendency of polymers at a particular temperature [20].

The crossover temperature, T_{cr}, is defined [18] as the temperature at which the rates of gas and char formation are equal, i.e., when $k_g = k_c$. From equation 26B

$$T_{cr} = \frac{(E_g - E_c)}{R \ln[A_g/A_c]} \tag{27}$$

It follows from equation 26A that the crossover condition, $k_g = k_c$, corresponds to an equilibrium char yield of 50%, i.e., $Y_c = 0.50$.

Substituting equation 26A into equation 25 yields the final result for the isothermal mass loss history in terms of the rate constant k_p for thermolysis of primary chemical bonds in the polymer,

$$\frac{m}{m_o} = Y_c + (1 - Y_c) \exp(-k_p t) \tag{28}$$

If $Y_c = \mu$ = constant, equation 28 is the solution for the isothermal mass loss history of a filled polymer with a nonvolatile mass fraction μ satisfying the rate law

$$\frac{dm}{dt} = -k_p (m - \mu m_o) \tag{29}$$

although equation 29 was not assumed *a priori* in the present derivation.

While estimation of the material parameters governing polymer pyrolysis is best accomplished under isothermal conditions as above, many processes of interest such as the production of combustible gases in a fire occur at finite heating rates. Consequently, it is important to be able to predict mass loss under dynamic heating conditions. For a constant heating rate, $\beta = dT/dt$, the independent variable in equation 28 can be transformed from time to the dimensionless variable

$$x = -k_p(T)\, t(T) = -\frac{A\,(T - T_o)}{\beta} \exp\left[-\frac{E_a}{RT}\right] \tag{30}$$

so that equation 28 can be written in the elementary form

$$\frac{m - m_o}{m_o} = (1 - Y_c) \int_0^{x_{max}} e^x\, dx \tag{31}$$

The exact solution of equation 31 for the fractional mass as a function of temperature at constant heating rate is

$$\frac{m\,(T)}{m_o} = Y_c + (1 - Y_c) \exp\left[-\frac{A}{\beta}\,(T - T_o)\, e^{-E_a/RT}\right] \tag{32}$$

Equation 32 is within 0.001% of the value obtained by double precision numerical integration of equation 31 over the temperature interval $T_o = 273$ K, $T = 1273$ K at 1 K increments after appropriate transformation of the independent variable from x to T.

The fractional mass loss rate during a linear temperature program is obtained by differentiating equation 32 with respect to time. No simple solution is possible when $Y_c = Y_c(T)$ so we make the drastic approximation that the equilibrium residual mass (char yield) is constant and independent of temperature, i.e., $Y_c = \mu$ and obtain

$$\frac{-1}{m_o}\frac{dm}{dt} = (1 - \mu)\, k_p(T) \left(1 + \frac{(T - T_o)\, E_a}{R\, T^2}\right) \exp\left[\frac{-(T - T_o)\, k_p(T)}{\beta}\right] \tag{33}$$

Noting that the maximum rate of change of m/m_o *versus* time/temperature occurs when $x = -1$, we set the exponent in equation 33 to -1 and obtain the useful approximation for the maximum mass loss rate of a polymer with inert fraction μ at constant heating rate

$$\left.\frac{-1}{m_o}\frac{dm}{dt}\right|_{T_{max}} \approx (1 - \mu)\, \frac{\beta\, E_a}{e R T_{max}^2} \tag{34}$$

where T_{max} is the temperature at peak mass loss rate obtained from the root of [32]

$$\ln\left[\frac{E_a}{RT_{max}}\right]^2 + \left[\frac{E_a}{RT_{max}}\right] + \ln\left[\frac{R\beta}{AE_a}\right] = 0 \tag{35}$$

EXPERIMENTAL

Anaerobic pyrolysis of 3-5 mg samples of low-density polyethylene ($M_w \approx 35{,}000$ g mol^{-1}, $M_w/M_n = 4.5$, and $\rho = 906$ kg m^{-3}, Aldrich Chemical), polymethylmethacrylate (PMMA, Aldrich Chemical, $M_w \approx 15{,}000$ g-mol^{-1}) and crosslinked phenolic triazine thermoset resin (PRIMASET PT 30, Lonza Chemical, or AROCY XU 371, Ciba Specialty Chemicals) were obtained under nitrogen (99.998% N_2, Matheson) flowing at 0.10 L min^{-1} in a thermogravimetric analyzer (Perkin Elmer TGA-7) after a 15-minute purge to remove residual air. Anaerobic, isothermal mass loss histories were recorded at temperatures ranging from 350–450°C for the phenolic triazine and nonisothermal scans were performed at selected constant heating rates ranging from 1 to 100 K/min for all materials. The polymethylmethacrylate and low-density polyethylene were used as received. The high-purity trifunctional cyanate ester novolac monomer was used as received without further purification and thermally cured without catalyst for four hours at 250°C to > 95% conversion as determined by infrared spectroscopy [33]. Curing the cyanate ester novolac monomer produces a tightly crosslinked thermoset network of oxygen-linked triazine rings (cyanurates) having the repeat unit atomic composition C_8H_5NO and the chemical structure

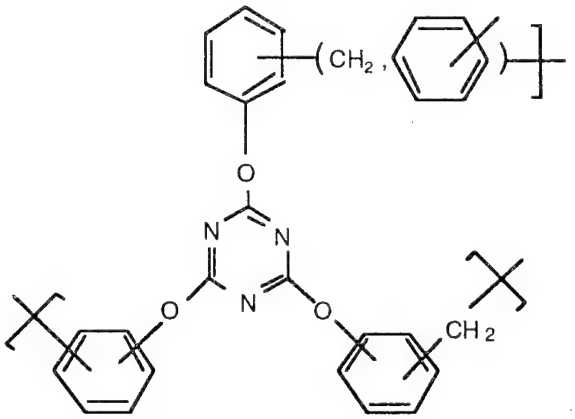

Experimental data for the isothermal mass loss histories of the cured phenolic triazine resin are shown as solid symbols in figure 4. Solid lines are the best fit of equation 28 to the experimental data using k_p and Y_c as adjustable parameters. Table 1 lists values for k_p and Y_c obtained from the fit of equation 28 to experimental data in figure 4. Figure 5 is an Arrhenius plot: $\ln(k_p) = \ln(A) - E_a/RT$ of the T and k_p values in table 1. The slope in figure 5 is E_a/R from which the activation energy is $E_a = 178$ kJ/mol. The intercept is the natural logarithm of the frequency factor for pyrolysis of the phenolic triazine, $A = 10^9$ sec^{-1}.

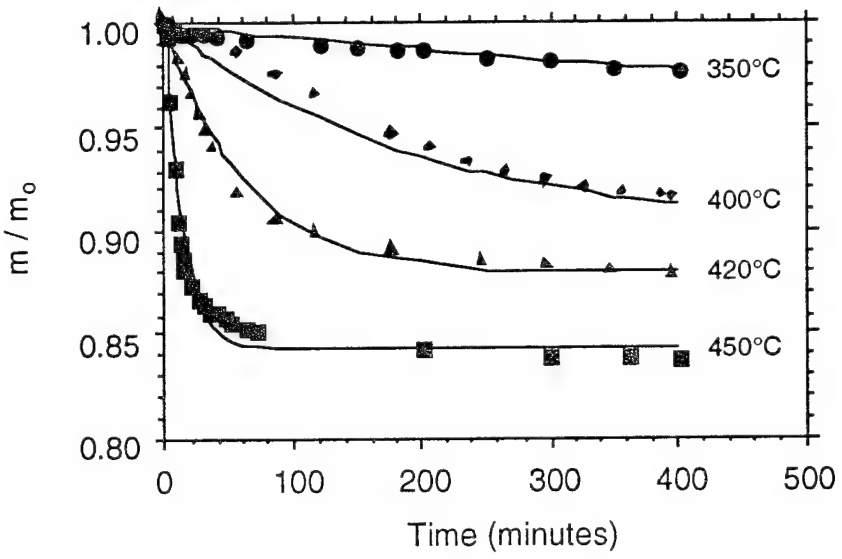

FIGURE 4. MEASURED AND CALCULATED ISOTHERMAL MASS LOSS HISTORIES AT INDICATED TEMPERATURES FOR PHENOLIC TRIAZINE RESIN. (Solid lines are fit of equation 28 using values for k_p and Y_c in table 1.)

It is important to recognize that both the activation energy and the frequency factor for pyrolysis obtained from the mass loss model for char forming polymers (28) are significantly lower than the values for these parameters obtained using generalized models for analysis of thermogravimetric data. For example, the Arrhenius parameters for k_p of the phenolic triazine resin obtained in this work (E_a = 178 kJ/mol, A = 10^9 sec^{-1}) compare to E_a = 280 – 326 kJ/mol and A = 10^{18} – 10^{20} sec^{-1} obtained from the same data using n-th order models [32, 33].

TABLE 1. BEST FIT k_P AND Y_c VALUES FOR PHENOLIC TRIAZINE THERMOSET RESIN

T (°C)	k_p (sec^{-1})	Y_c
350	1.4 x 10^{-5}	0.92
400	8.5 x 10^{-5}	0.90
420	2.7 x 10^{-4}	0.88
450	1.2 x 10^{-3}	0.84

The relative rate constants for volatile and char formation are obtained by plotting equation 26B in the form

$$\ln\left[\frac{1-Y_c}{Y_c}\right] = \ln\left[\frac{A_g}{A_c}\right] - \left[\frac{E_g - E_c}{R}\right]\frac{1}{T} \qquad (36)$$

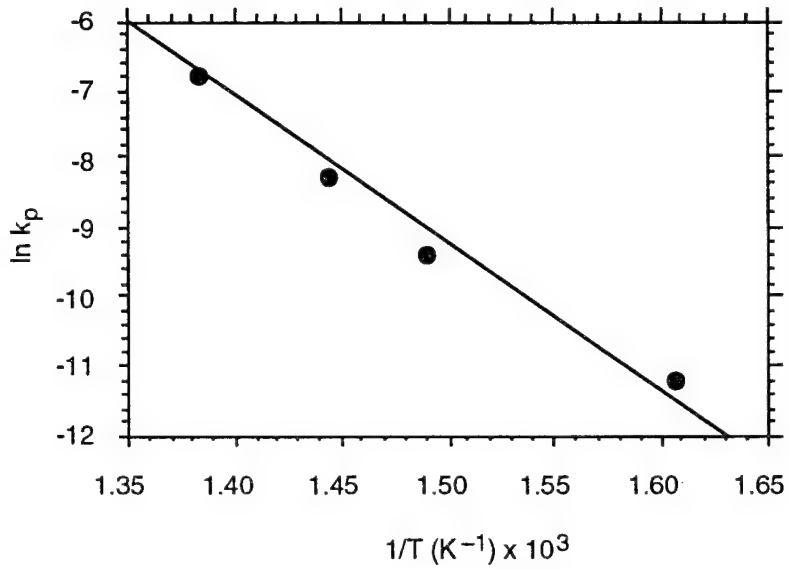

FIGURE 5. PLOT OF THE NATURAL LOGARITHM OF k_p VERSUS RECIPROCAL TEMPERATURE FOR PHENOLIC TRIAZINE RESIN

Thus, a plot of $\ln[(1-Y_c)/Y_c]$ versus 1/T has a slope proportional to the difference in activation energies for volatile and char formation and an intercept which is the natural logarithm of the ratio of the frequency factors. Figure 6 shows a plot of equation 36 using the isothermal char yields in table 1. The slope gives $E_g - E_c = +30$ kJ/mol and the intercept $A_g/A_c = 17$. This result indicates that even though the molecular collision frequency for gas production is seventeen times greater than for char formation, char formation has a lower activation energy by 30 kJ/mol which is perhaps due to resonance stabilization of the polycyclic aromatic char [34]. The Arrhenius parameters for gas and char formation substituted into equation 26B allow calculation of the equilibrium char yield as a function of temperature. The crossover temperature for the phenolic triazine resin from equation 27 is

$$T_{cr} = \frac{(30\ \text{kJ/mol})}{R\ \ln[17]} = 1273\ \text{K}$$

For the phenolic triazine resin the rates of primary char and volatile formation are equal at 1000°C and $Y_c = 0.50$. In comparison the crossover temperature for cellulose is about 250°C from char yield data and the criteria $Y_c = 0.50$ [9].

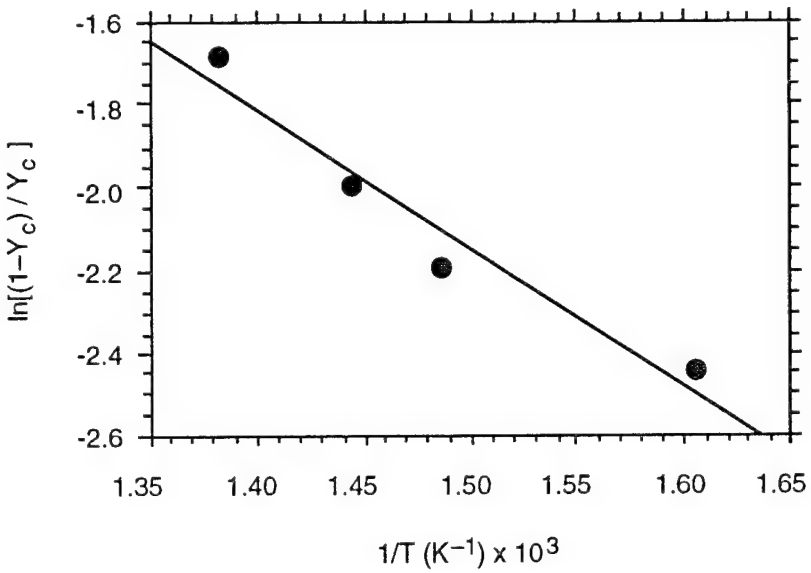

FIGURE 6. PLOT OF THE NATURAL LOGARITHM OF $(1-Y_c)/Y_c$ VERSUS RECIPROCAL TEMPERATURE FOR PHENOLIC TRIAZINE RESIN

The predicted mass loss of the phenolic triazine resin at constant heating rates of β = 1, 5, and 20 K/min calculated from equation 32 is compared to thermogravimetric data in figure 7. The parametrically determined $A = 10^9$ sec^{-1}, E_a = 178 kJ/mol, and the temperature dependent char yield $Y_c(T)$ from equation 26B were used in the calculations. Solid symbols are the thermogravimetric data at the indicated heating rates. Solid lines are the predictions of equation 32 for those same heating rates, and the dotted line is the equilibrium char yield corresponding to $\beta = 0$.

Agreement between the measured and calculated residual mass of the phenolic triazine resin in the scanning TGA experiments is generally good for temperatures below about 700°C as shown in figure 7. The difference between the model and the experimental data above 700°C at these heating rates is a result of neglecting secondary charring and gasification in the simplified mass loss model which considered only primary char and gas formation (Assumption C).

Equation 32 was used to predict mass loss curves for the phenolic triazine resin at the high heating rates $\beta \approx 1$ to 100 K/s characteristic of a burning polymer in a fire [31]. Figure 8 shows these calculations for five decades of heating rate ranging from $\beta = 0.01$ to 100 K/s. Figure 8 shows that both the temperature at maximum mass loss rate, T_{max}, and the volatile mass fraction, $m/m_o - Y_c(T_{max})$, increase significantly with heating rate for a charring polymer as the material becomes superheated.

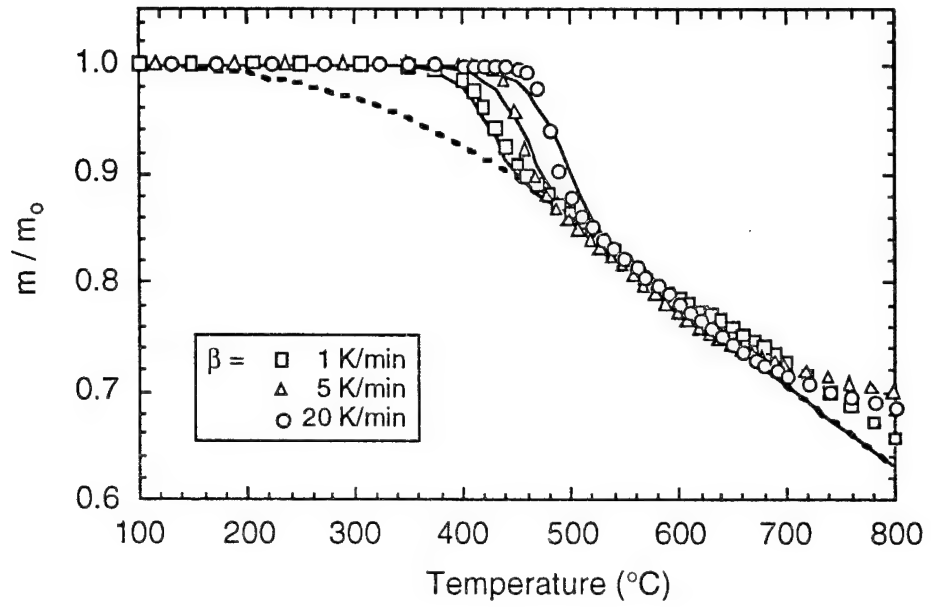

FIGURE 7. COMPARISON OF MEASURED AND CALCULATED MASS LOSS OF PHENOLIC TRIAZINE RESIN IN THERMOGRAVIMETRIC ANALYZER AT CONSTANT HEATING RATES OF β = 1, 5, AND 20 K/min. (Solid lines are fit of equation 32 to experimental data for indicated heating rates. Dashed line is calculated equilibrium char yield (β = 0) versus temperature.)

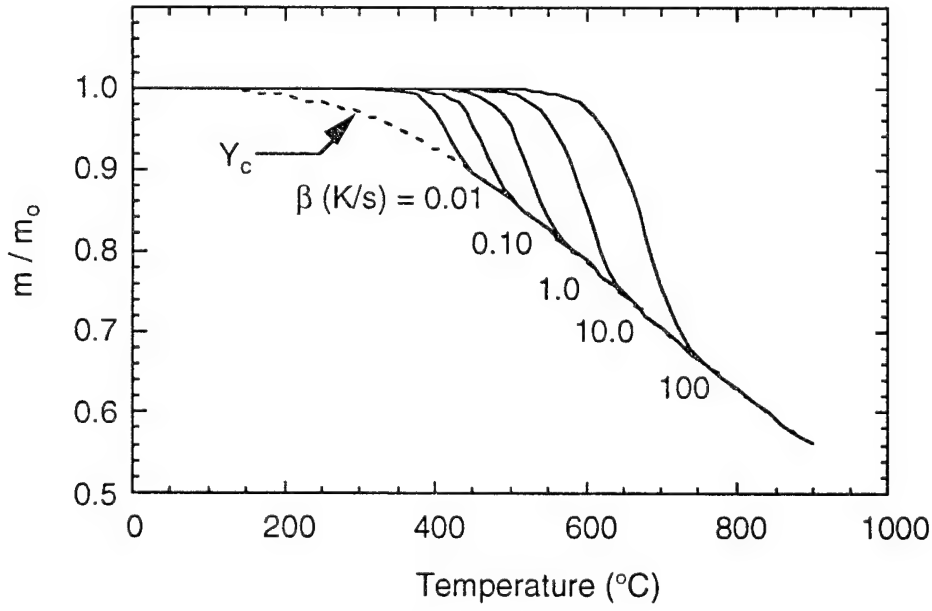

FIGURE 8. MASS LOSS CALCULATIONS FOR PHENOLIC TRIAZINE RESIN AT FIVE DECADES OF HEATING RATE

Table 2 compares measured and calculated peak fractional mass loss rates at various heating rates for the noncharring polymers PMMA and polyethylene and the char-forming phenolic triazine resin. Calculated values were obtained using equation 34 with the indicated heating rates. For the phenolic triazine with E_a = 178 kJ/mol, a value of $\mu = 0.75 = Y_c$ (650°C) gave the best fit of the peak mass loss rate data. For the polymethylmethacrylate of this study, E_a = 160 kJ/mol [32, 35] and $\mu = 0$, while for low-density polyethylene, E_a = 200 kJ/mol [35, 36] and $\mu = 0$. The average error in the calculated peak mass loss rates is about ± 30% of experimental values which is on the order of the uncertainty in the activation energies used in the calculation. Thus, equation 34 qualitatively describes the peak mass loss rate of charring and noncharring polymers over a wide range of constant heating rates. This result could explain the lower heat release rate of polymers with high decomposition temperature and char yield in terms of the mass loss (fuel generation) rate in the pyrolysis zone during flaming combustion.

TABLE 2. MEASURED AND CALCULATED PEAK MASS LOSS RATES FOR POLYMETHYLMETHACRYLATE, POLYETHYLENE, AND PHENOLIC TRIAZINE POLYMERS

Heating Rate	T_{max} (measured)	Peak Mass Loss Rate (measured)	Peak Mass Loss Rate (calculated)
K/min	Kelvin	mg/g-s	mg/g-s
PHENOLIC TRIAZINE			
1	693	0.03	0.07
3	703	0.14	0.20
5	724	0.29	0.31
10	743	0.63	0.59
20	745	1.28	1.18
POLYMETHYLMETHACRYLATE			
3	639	1.38	1.03
10	653	3.81	3.32
30	682	10.03	9.65
100	698	28.63	31.11
200	719	47.65	61.03
POLYETHYLENE			
3	738	1.89	0.81
10	757	5.55	2.63
30	778	14.27	7.31
100	790	26.38	23.68
200	808	63.50	45.14

CONCLUSIONS

The objective of this work was to obtain analytic solutions for the mass loss and mass loss rate of char forming polymers from a mechanistic pyrolysis model to provide insight into the fuel generation process during flaming combustion. Analytic solutions for the residual mass having a minimum number of adjustable parameters were desired so that the model could be easily evaluated for different materials on conventional thermogravimetric equipment. A mechanistic pyrolysis model for cellulose pyrolysis provided rate equations for volatiles and char which reduced to a single first-order rate law for the isothermal mass by making the reasonable assumptions: (1) primary-bond dissociation is the rate-limiting first step, (2) mass loss proceeds through an active intermediate which is a stationary state, (3) primary gas and char production are competing processes whose magnitude and rate constants are large compared to successive products and rate processes, and (4) conditions are anaerobic. Exact results were obtained for the isothermal mass

loss history of a char forming polymer which included an equilibrium char yield whose value depends only on temperature through the relative rates of gas and char formation. In the present analysis, the crossover temperature at which rates of gas and char formation are equal corresponds to the temperature at which the equilibrium char yield is 50%.

Comparison of the model prediction with the measured mass loss history of a phenolic triazine thermosetting resin in temperature scanning thermogravimetric experiments showed excellent agreement for the first stage of thermal decomposition to volatiles and char. An approximate expression for the maximum mass loss rate at constant heating rate was derived which is in qualitative agreement with thermogravimetric data for charring and noncharring polymers. The simple analytic solution for peak mass loss rate during steady heating shows that the maximum fuel generation rate decreases linearly with char yield and is inversely proportional to the square of the (rate dependent) peak decomposition temperature. Thus, the analytic result for mass loss in a relatively complex polymer thermal decomposition process is physically based with temperature and heating rate dependent product yields which are important in fire modeling (e.g., volatile and char formation). Although outside the scope of the present work, the incorporation of thermoxidative processes in the global thermal degradation scheme (equations 6-8) allows for a more detailed analysis of the mass loss rate of polymers heated under aerobic conditions.

REFERENCES

1. Babrauskas, V. and Peacock, R.D., Fire Safety Journal, 1992, **18**, 255.

2. Demarco, R.A. , Proc. 36th Int'l. SAMPE Symposium, 1991, April 15-18, 1928.

3. Hathaway, W.T., Proc. 36th Int'l. SAMPE Symposium, April 15-18, 1991, 1900.

4. Hill, R.G., Eklund, T.I., and Sarkos, C.P. "Aircraft Interior Panel Test Criteria Derived from Full-Scale Fire Tests," 1985, DOT/FAA/CT-85/23.

5. Van Krevelen, D.W., "Properties of Polymers," Chapter 26B, Flammability of Polymers, Elsevier Scientific, NY, 1976.

6. Bassett, W., Proc. Fire Retardant Chemicals Association Meeting, San Antonio, TX, March 12-15, 1989.

7. Factor, A., "Fire and Polymers: Hazards Identification and Prevention," G.L. Nelson, ed., ACS Symposium Series, **425**, American Chemical Society, Washington, D.C., 1990.

8. Shafizadeh, F. and Chin, P.P.S., ACS Symposium Series, American Chemical Society, Washington, D.C., **43**, 1977.

9. Broido, A. and Nelson, M.A., Combustion and Flame, 1975, **24**, 263.

10. Antal, M.J., Jr. and Varhegyi, G., I&EC Res., 1995, **34**, 703.

11. Shafizadeh, F., Adv. Carbohydrate Chem., 1968, **23**, 419.

12. Milosavljevic, I. and Suuberg, E.M., 1995, Ind. Eng. Chem. Res., **34**, 1081.

13. Lewellen, P.C., Peters, W.A., and Howard, J.B., 1976, Proc. 16th Symposium (Int'l.) on Combustion, The Combustion Institute, 1471.

14. Welker, J. R., J. Fire and Flammability, 1970, **1**, 12.

15. Suuberg, E.M., Milosavljevic, I., and Vahur, O., 1996, Proc. 26th Symposium (Int'l.) on Combustion, The Combustion Institute, 1515.

16. Di Blasi, Comb. Sci. and Tech., 1993, **90**, 315.

17. Wichman, I.S. and Atreya, A., Combustion and Flame, 1987, **68**, 231.

18. Wichman, I.S. and Oladipo, A.B., Proc. 4th Int'l. Symp. Fire Safety Sci., 1994, Int'l. Assoc. Fire Safety Science, 313.

19. Wichman, I.S. and Melaaen, M., in "Advances in Thermochemical Biomass Conversion," T. Bridgewater (ed.) Champman and Hall, London, 1993.

20. Van Krevelen, D.W., Polymer, 1975, **16**, 61520.

21. Lengele, G., AIAA J., 1970, **8**(11), 1989.

22. Van Krevelen, D.W., "Properties of Polymers," Ch. 21, Thermal Decomposition, Elsevier Scientific, NY, 1976.

23. Wolfs, P.M.J., Van Krevelen, D.W., and Waterman, H.I., Brennstoff Chemie, 1959, **40**, 155.

24. Carty, P. and White, S., Polymer, 1994, **35**(2), 343.

25. Ponder, G.R., Richards, G.N., and Stevenson, T.T., J. Anal. Pyro., 1992, **22**, 217.

26. G. Odian, Principles of Polymerization, 2nd Edition, Wiley-Interscience, N.Y. pp. 268-271, 1981.

27. Milosavljevic, I., Oja, V., and Suuberg, E.M., 1996, Ind. Eng. Chem. Res., **35**, 653.

28. Friedman, H.L., J. Polym. Sci.:C, 1962, **6**, 183.

29. Nam, J.D. and Seferis, J.C., J. Polym. Sci.:B, 1992, **30**, 455.

30. Wall, L.A., in "Flammability of Solid Plastics," **7**, Fire and Flammability Series, Technomic Publ., Westport, CT, 323, 1974.

31. Beyler, C.L. and Hirschler, M.M., SFPE Handbook of Fire Protection Engineering, 2nd Edition, Section 1.1.7, National Fire Protection Association, Boston, MA, 1995.

32. Lyon, R.E., in "Fire and Polymers II," G.L. Nelson, ed., ACS Symposium Series 599, American Chemical Society, Washington, D.C., 618, 1995.

33. Lyon, R.E., Arnold, F.E., Rodriguez-Arnold, J., Granville, A., and Das, S., Proc. Fire Retardant Chemicals Association Meeting, Williamsburg, VA, October 9-12, 1994.

34. A. Factor in "Fire and Polymers," G.L. Nelson, ed., ACS Symposium Series 425, American Chemical Society, 274, 1990.

35. N. Grassie and A. Scotney in Polymer Handbook, 2nd Edition, J. Brandrup and E.H. Immergut, eds., II-467, Activation Energies for the Thermal Degradation of Polymers, Wiley Interscience, NY, 1975.

36. Lyon, R.E., Thermochimica Acta (in press).